Effect of daily setup errors on individual dose distribution in conventional radiotherapy: an initial study

Title

Effect of daily setup errors on individual dose distribution in conventional radiotherapy: An initial study

Names

Akihiro Takemura, Saori Shoji*, Sinichi Ueda*, Yuichi Kurata*, Tomoyasu Kumano**, Shigeyuki Takamatsu**, Masayuki Suzuki

Division of Health Sciences, Graduate School of Medical Science, Kanazawa University

5-11-80 Kodatsuno, Kanazawa 920-0942, Japan

*Kanazawa University Hospital

1-13 Takaramachi, Kanazawa 920-8641, Japan

**Department of Radiology, Graduate School of Medical Science, Kanazawa University

1-13 Takaramachi, Kanazawa 920-8641, Japan

Concise and informative title

Effect of daily setup errors on the individual dose distribution

Corresponding author

Akihiro Takemura

Email: at@mhs.mp.kanazawa-u.ac.jp Telephone: +81-76-265-2538

Fax:+81-76-234-4366

Abstract

Recent linear accelerators can perform cone beam computed tomography to correct setup errors immediately before dose delivery. We calculated the dose distribution with setup errors acquired from cone-beam computed tomography to determine a more realistic and individual effect of setup errors. The differences in dose distribution were analyzed. The setup errors of three patients who were irradiated in the neck, esophagus, and pelvic area were obtained retrospectively. We found that the maximum dose variances for the three cases were 19.9 to 35.9%. The maximum dose variance points were relatively far from the isocenter. The volume of the 10% dose difference had widths of 1.3 to 1.85 cm around the beam edges. The V95 and mean doses at the clinical target volume were mostly unchanged. Doses around the beam edges were more varied than those around the isocenter for every case. The dose on the spinal cord located near the beam edges varied by 5 – 10 % compared with the dose of the radiotherapy plan in two of the cases. We demonstrated the individual dose distributions of the cases affected by daily setup errors for all fractions.

Keywords

Radiotherapy, Setup error, Dose distribution, Image-guided radiotherapy, Cone-beam CT

Introduction

Setup errors at each fraction of radiotherapy can cause dose variation within the body, and thus an unexpected underdose to a tumor and/or an overdose of radiation to normal tissue may be delivered. American Association of Physicists in Medicine Report 13 [1] states that the spatial uncertainty of external radiotherapy should be smaller than 10 mm and that the patient setup error of this spatial uncertainty should be smaller than 6 mm. More accurate patient localization is currently required in stereotactic irradiation. Methods for measuring setup errors have been developed, and registration methods for their correction have been developed.

In a previous study, setup errors were measured in patients who underwent irradiation of the whole pelvic area, by use of a portal image and a digitally reconstructed radiograph (DRR). The DRR was reconstructed from computed tomography (CT) images [2]. In another study, setup errors were examined in patients whose livers were irradiated with stereotactic body radiation therapy [3]. Several authors have described registration methods for two-dimensional to three-dimensional (2D-3D) volume data, produced with standard or cone-beam computed tomography (CBCT) and a portal image for setup error assessment [4-8]. Létourneau et al. [9] measured setup errors by using 3D-3D registration of CT volume data and CBCT volume data.

Several studies have estimated the effects of setup errors on the dose distribution. Wang et al. [10] used computer simulation to describe the effects of setup errors in the treatment of spinal metastases with stereotactic body radiotherapy. Setup error effects have also been described in intensity-modulated radiation therapy (IMRT) for head and neck

tumors [11, 12]. However, the results from both of these studies showed the averaged effects and did not explain the effects on dose distribution for individual patients. Using computer simulation involving estimated values of errors and variance gives only an estimation of the effects of setup errors.

The effects of actual setup errors have been calculated in three separate studies. In two of these studies [13, 14], setup error data were obtained by use of portal images or radiographs with on-board imaging systems. The images in these studies were 2D, and thus only the translational setup error was taken into account. Rotational error is a separate the component of setup error. Schaly et al. [15] used CT images taken frequently during the treatment course. CT sessions were performed up to 15 times in 77 fractions per case (i.e., measurements were not made at all fractions). In another study [16], setup errors were obtained by use of CT images and a portal image for development of a mathematical model. The difference in the biological effective dose (BED) was then calculated. The effect of random error in the patient setup on the BED has also been calculated previously [17].

Many studies have focused on examining the broad effects of setup errors in order to determine the margins of their sufficient planning target volume (PTV). We believe that clarifying the effects of daily setup errors on the individual dose distribution is important because the dose distribution may reveal setup-error-induced overdose and could potentially inform the prediction of side effects of the treatment course. Our overarching goal is to develop a system for calculating realistic and individual-specific setup error effects on the dose distribution for post-treatment assessment.

In this study, we verified the calculability of the effects of setup errors for all

fractions obtained from an image-guided radiotherapy (IGRT) system. Moreover, we wanted to determine the usefulness of calculating the effects of setup errors on the dose distribution for post-dose assessment. We obtained daily setup errors for all fractions by using a 3D-3D registration of CT volume data and CBCT volume data acquired immediately before irradiation. In this initial study, we selected three cases. One involved irradiation of the chest, one of the head and neck, and one of the pelvic area.

Materials and Methods

We used a linear accelerator (Linac) integrated with an X-ray and flat panel detector (FPD) system (Elekta Synergy, Elekta AB, Stockholm, Sweden). The X-ray and FPD system was mounted on the gantry system of the Linac, and the beam directions of the Linac and of the X-ray and FPD systems were orthogonal to each other.

The X-ray and FPD system is able to perform CBCT and provide 3D volume data on a patient immediately prior to irradiation. The CBCT volume data are typically registered immediately with the CT volume data of the radiotherapy plan for calculation of errors in patient positioning. The couch is then moved to correct these errors.

Using this system, we measured setup errors consisting of translational errors for each patient in the X, Y, and Z directions, and rotational errors for each patient around each axis. Systematic components (mean) and random components (standard deviation) of the setup errors for each axis and each case are shown in Table 1. The X-axis indicates the lateral direction (right to left), the Y-axis indicates the longitudinal direction (inferior to superior), and the Z-axis indicates the vertical direction (posterior to anterior) of the patient

(Figure 1). CBCT and registration are performed routinely at every dose fraction in the hospital. Setup error data were obtained retrospectively. A small field of view (270 mm in diameter in the XY plane and 264 mm in the Z axis; a 512 x 512 x 512 matrix) was used for all acquisitions. The algorithm of registration was bone-matching, which uses the bone structure of the patient to calculate positional errors.

To ascertain the effects of daily setup errors on the dose distribution, we developed a radiotherapy plan that included setup errors. This plan was constructed from the approved plan, which was used for the actual treatment. All beams in the approved plan were duplicated for every fraction. For example, if the approved plan had four beams and 20 fractions, a plan with 80 beams was designed. Alignment of all beams was rearranged for producing daily setup errors. The beam alignment was calculated by use of a transformation between the orthogonal coordinate system and the spherical coordinate system and affine transformation. The gantry angle and couch angle were used as components in a spherical coordinate system with origin at the isocenter. The tilt angle was used for the gantry angle, and the azimuth angle stood for the couch angle. Setup errors were the components in an orthogonal coordinate system.

The translational errors of a setup error can be represented by shifting of the isocenter. The rotational setup errors were represented by variation of the gantry angle, couch angle, and collimator angle. The rearranged gantry angle θ', couch angle ϕ', and collimator angle ω' were calculated from the original gantry angle θ, couch angle ϕ, and collimator angle ω of the approved plan, as described in the following paragraphs.

First, the source position in a spherical coordinate system, represented by the

source-isocenter distance *r* and the original gantry angle θ and couch angle ϕ, was transferred to orthogonal coordinates. This calculation was defined as follows;

$$S\begin{pmatrix} x \\ y \\ z \end{pmatrix} = \begin{pmatrix} r\sin\theta\cos\phi \\ r\sin\theta\sin\phi \\ r\cos\theta \end{pmatrix} \quad \text{---------- (1)}$$

Vector *S* of the source position was in the orthogonal coordinate system. The normal vector *C* of the plane including the *S* and Z axes was also determined for the calculation of a collimator angle ω'. Vectors *S* and *C* were then transformed by the affine transformation to produce rotational setup errors. *T* is a transfer matrix, and the affine transformation was calculated as follows:

$$S'\begin{pmatrix} x_s' \\ y_s' \\ z_s' \end{pmatrix} = T \cdot S\begin{pmatrix} x_s \\ y_s \\ z_s \end{pmatrix} \quad \text{----------(2)}$$

$$C'\begin{pmatrix} x_c' \\ y_c' \\ z_c' \end{pmatrix} = T \cdot C\begin{pmatrix} x_c \\ y_c \\ z_c \end{pmatrix} \quad \text{----------(3)}$$

The coordinate system as shown in Figure 1 was defined as follows:

$$T = \begin{pmatrix} \cos R_z & -\sin R_z & 0 \\ \sin R_z & \cos R_z & 0 \\ 0 & 0 & 1 \end{pmatrix}\begin{pmatrix} \cos R_y & 0 & \sin R_y \\ 0 & 1 & 0 \\ -\sin R_y & 0 & \cos R_y \end{pmatrix}\begin{pmatrix} 1 & 0 & 0 \\ 0 & \cos R_x & -\sin R_x \\ 0 & \sin R_x & \cos R_x \end{pmatrix} \quad \text{--------- (4)}$$

where R_x, R_y, and R_z are the rotational errors of the X, Y, and Z axes at a fraction, respectively. *S'(x'$_s$, y'$_s$, z'$_s$)* was a source position producing rotational setup errors in the orthogonal coordinate system. This was transferred to coordinates in the spherical coordinate system as follows:

$$\theta' = \tan^{-1}\left(\frac{\sqrt{x_s'^2 + y_s'^2}}{z'}\right) \quad \text{----------(5)}$$

$$\phi' = \tan^{-1}\left(\frac{y_s'}{x_s'}\right) \quad \text{----------(6)}$$

We obtained the rearranged gantry angle θ' and couch angle ϕ'. The collimator angle ω' was defined as

$$\omega' = \omega + \Delta\omega \quad \text{----------(7)}$$

where $\Delta\omega$ is an angle between *C'* and the normal vector *N* of the plane including *S'* and the Z axis. $\Delta\omega$ can be calculated by the dot product of *C'* and the normal vector *N* as

$$\cos\Delta\omega = \frac{C' \cdot N}{|C'||N|} \quad \text{----------(8)}$$

Finally, the gantry angle θ', the couch angle ϕ', and the collimator angle ω' were calculated.

We used a radiotherapy planning system (RTPS), Xio Release 4.3.1 (CMS Inc., St. Louis, Missouri, USA), to build the radiotherapy plan. The superposition method was used as a dose calculation algorithm. The RTPS included a maximum beam-number constraint of 99 beams. Therefore, we had to select cases where the product of the number of beams and the number of fractions was within this constraint.

In this study, we retrospectively obtained setup error data from three patients, one who was irradiated in the neck, one in the esophagus, and one in the coccygeal bone area (a 62 year-old man, a 74 year-old man, and a 50 year-old woman, respectively) as initial cases. We purposely chose one patient for each irradiated site in the head and neck, chest, and

abdomen or pelvic area. We did not select patients with lung or abdominal tumors, in order to avoid potential respiratory motion. Whole pelvic irradiation is not performed with the Linac because the maximum field size of the multileaf collimator (21 cm x 16 cm) is not sufficiently large to cover the necessary area for the procedure. Another Linac at our institution is able to perform whole pelvic irradiation, but CBCT is not performed at every fraction.

We obtained CBCT registration results for setup error data from the three patients. The patients treated in the neck, esophagus, and coccygeal bone were respectively labeled cases A, B, and C. Case A was irradiated with oblique parallel opposing fields (1^{st} port 315 degrees, 2^{nd} port 135 degrees) with 15 degree wedges, and he was immobilized with a head and neck shell (ESS-24, Engineering System Co. Ltd., Japan). The number of fractions was 30, and the total dose was 6000 cGy (6 MV X-rays). Case B was irradiated with oblique parallel opposing fields (1^{st} port 320 degrees, 2^{nd} port 140 degrees) without wedges and with an arm support pillow (ESF-18, Engineering System Co. Ltd., Japan). The number of fractions was 10, and the total dose was 2000 cGy (10 MV X-rays). Case C was irradiated with cross-fire fields (1^{st} port 0 degrees, 2^{nd} port 90 degrees, 3^{rd} port 180 degrees, 4^{th} port 270 degrees), and the 3^{rd} and 4^{th} ports had a 20-degree wedge filter added, and a heel support pillow (ESS-38, Engineering System Co. Ltd., Japan) was used. The number of fractions was 20, and the total dose was 6000 cGy (10MV X-ray). The Linac comes with a motorized wedge system with an adjustable wedge angle.

The beam isocenter was placed at the center of the clinical target volume (CTV), which was delineated by radiation oncologists. The dose was normalized by the dose at the

isocenter. The multi-leaf collimator (MLC) leaf position is typically determined by the volume, which is derived from the CTV plus the PTV margin of 5 mm and MLC margin of 5 mm (total, 10 mm). The MLC leaf position, however, is sometimes adjusted according to the particular case. In the radiotherapy plan for case C, the MLC margin was increased to 10 mm. For cases A and B, only CTV was delineated and the MLC leaf position was determined by addition of a 10 mm margin (5 mm PTV margin + 5 mm MLC margin) to the CTV. A summary of the three cases is shown in Table 1, and the beam alignment of their approved plans is shown in Figure 2.

We calculated the dose distribution of the plan with setup errors, then subtracted the dose distribution of the approved plan. This allowed us to determine the difference between the two dose distributions, giving the effect of setup errors. In the differential dose distribution, we measured the maximum width of the differential iso-dose cross-sections at 10% difference, as well as the maximum dose difference. The dose expressed as a percentage in the differential dose distribution was based on the total dose (i.e., 6000 cGy for cases A and C and 2000 cGy for case B). The width of the differential iso-dose cross-section at 10% difference was orthogonal to the beam direction. The width was measured at several depths along each beam, and the maximum width was obtained. The maximum dose difference was calculated as the maximum variation between the dose distributions of the approved plan and those of the plan with setup errors.

Dose-volume histograms (DVHs) of the CTV and organs at risk (ORs) of the plans with the setup errors were compared with those of the approved plans. The volume covered by 95% or more of the dose (the V95), and the mean dose of the CTV were calculated for

each case.

Results

Figure 3 shows the dose distributions of the approved plans, the plans with setup errors, and the subtractions of these dose distributions in each case. The slices in the figure were chosen because they showed a relatively large dose variation. The dose distributions for the approved plan and the plan with setup errors appeared similar to each other, but in the differential dose distribution, dose variation appeared along the beam edges. A region of 5–10% dose difference overlapped in a part of the spinal cord in cases A and B.

The maximum dose differences were 34.7% for case A, 35.9% for case B, and 19.9% for case C. The maximum dose difference point was located on the beam edge, relatively far from the isocenter. The maximum widths of the differential iso-dose cross-sections at 10% difference were 1.7 cm, 1.6 cm, and 1.3 cm for cases A, B, and C, respectively.

The DVHs for the CTV in the plan with the setup errors for all three cases were similar to those of the approved plan. The DVH for the PTV in the plan with setup errors for case C was decreased slightly from that of the approved plan (Figure 4). The results of the V95 and mean dose are shown in Table 2. The differences of V95s of CTV between the approved plan and the plan with setup errors were 1.9%, 0.4%, and 0.1% for cases A, B, and C, respectively (7.8% for the PTV in case C). The differences in mean doses of the CTVs between the approved plan and the plan with setup errors were 0.5%, 0.3%, and 0.4% for cases A, B, and C, respectively (0.8% of PTV in case C). No major differences

were found in the V95 and mean dose between the plans. The DVH for the spinal cord in the plan with setup errors for case B (located near the CTV) was slightly increased from that in the approved plan because of dose variation around the beam edges.

The maximum dose points in the differential dose distributions, where the dose varied the most, were located along the beam edge, far from the isocenter (Figure 5).

Discussion

We found that the dose for the CTV was not greatly affected by the setup error. This finding can be explained in the following way. First, the rotational potion of the setup error would be expected to change the dose more in parts of the body located far from the isocenter than doses around the isocenter (i. e., the CTV was located around the isocenter). The translational error would, in turn, be expected to affect the dose of the beam edges because the dose intensity in the fields was uniform. If the analysis used in this study is applied to the dose distribution for the IMRT plan, the dose for a target may be changed.

The V95 of the CTV for case C was higher than that for the other cases, and the difference between the V95s for the approved plan and the plan with setup errors was small. The most likely reason for the high V95 in case C is the wider MLC margin in case C compared with the other cases. However, the V95 of the PTV for case C was decreased by approximately 8% in the plan with setup errors compared with the approved plan. We believe that a small PTV volume caused a decrease in the V95. If the dose-modified volume in a PTV is small, and a PTV is large enough, the V95 would not be expected to change substantially. On the other hand, if a PTV is small, the V95 may change by a large

amount. Case C had a small PTV that was less than one quarter of the CTV for case A. Thus the V95 of PTV for case C could have been more sensitive than that for the other cases. However, differences in the mean dose and V95 of the CTV between the approved plan and the plan with setup errors were small, and thus the dose to the CTV was largely unaffected by setup errors.

Rotational errors may have the largest effect on the dose variation at large distances from the isocenter. The position of the maximum dose difference was far from the isocenter. This suggests that an OR far from the isocenter and close to the beam edge could receive an unexpectedly high dose (approximately 35% higher according to the results of this study) due to setup errors in traditional radiotherapy without an image-guided system.

On the other hand, translational errors could cause the dose around a target to vary. The dose of an OR near a target was found to vary by 5-10% from doses in the approved plan (e.g., cases A and B). A part of the spinal cord in case A happened to be covered by a -5% iso-dose line. However, the spinal cord may still receive higher doses according to setup errors. When the plan is changed to avoid exceeding the tolerance dose of the OR, the volume of the OR plus a sufficient margin (i.e., planning organ at risk volume) should be defined to avoid an overdose. We found that the 10% dose region in the differential dose distributions had a 1.3 to 1.85 cm width around the beam edges.

The dose distribution difference is likely to depend on the magnitude of the systematic setup errors. However, this is not illustrated clearly by our results. Of the three cases, case B had the largest maximum rotational error magnitude (a rotational error of 2.32 degrees for the X axis), and case A had the next highest value. This ranking of the

magnitude of the rotational error is equal to the ranking of the magnitude of the maximum dose in the differential dose distributions. However, the ranking of the magnitude of the translational error did not match the ranking of the magnitude of the rotational error.

The magnitude of the setup errors in this study was the same as that reported in previous studies [1-3, 5, 9, 11, 13]. Thus, we believe that dose distribution variation, such as the variation shown in the present results, is generally present in traditional radiotherapy treatment. Index values such as the V95 and mean dose may be affected by the volume and location of a tumor and the irradiation technique. Future studies involving a greater number of cases will be required for further clarification of the effects of setup errors. In addition, internal organ motion and non-rigid deformation of the body were not taken into account in this study because they cannot be measured with the Linac system. However, motion and deformation may strongly affect the dose distribution, and thus they should be considered in future studies.

In our hospital, a bone-matching algorithm is used for CT-CBCT registration to correct a patient's setup because the alternative algorithm, intensity matching, is highly time-consuming, involving approximately 10 - 20 minutes per patient. Thus, our setup error data, which were obtained retrospectively, were provided by registration with the bone-matching algorithm. This registration does not always give the true setup error. Feature-based registration algorithms, such as the bone-matching algorithm, are not always robust. However, our preliminary study found that the bone-matching and intensity-matching algorithms were similarly robust. In addition, we believe that 0.5 degrees (the maximum angular difference between an actual angle and a rounded value of

the angle) was too small to produce a large difference in a dose distribution. Overall, we were able to calculate the individual dose distribution by taking daily setup errors into account in each case, and to assess the dose distribution.

Conclusion

We were able to calculate dose distributions affected by actual setup errors of entire fractions for three patients undergoing radiotherapy. We were able to assess the dose distributions of the radiotherapy plan with setup errors and found the following: the setup errors affected the dose around the beam edges; the DVHs, V95s, and the mean doses for the CTVs were mostly unchanged, and a part of the spinal cord in two of the cases received a dose that was changed by 5 – 10% in the plan with setup errors.

References

1. AAPM, Dosimetric accuracy and equipment tolerances. In: AAPM Report 13 Physical aspects of quality assurance in radiation therapy. Huston Texas: AAPM; 1984. p. 7-13

2. Haslam JJ, Lujan AE, Mundt AJ, Bonta DV, Roeske JC. Setup errors in patients treated with intensity-modulated whole pelvic radiation therapy for gynecological malignancies. Med Dosim. 2003; 30: 36-42.

3. Dawson LA, Eccles C, Bissonnette JP, et al. Accuracy of daily image guidance for hypofractionated liver radiotherapy with active breathing control. Int J Radiat Oncol Biol Phys, 2005; 62(4): 1247-52

4. Kunzler T, Grezdo J, Bogner J, Birkfellner W, Georg D. Registration of DRRs and portal

images for verification of stereotactic body radiotherapy: a feasibility study in lung cancer treatment. Phys Med Biol. 2007; 52: 2157-70.

5. Clippe S, Sarrut D, Malet C, Miguet S, Ginestet C, Carrie C. Patient setup error measurement using 3D intensity-based image registration techniques. Int J Radiat Oncol Biol Phys. 2003; 56: 259-65.

6. Jans HS, Syme AM, Rathee S, Fallone BG. 3D interfractional patient position verification using 2D-3Dregistration of orthogonal images. Med Phys. 2006; 33: 1420-39.

7. Munbodh R, Jaffray DA, Mosely DJ, Chen Z, Knisely JP, Cathier P, et al. Automated 2D-3D registration of a radiograph and a cone beam CT using line-segment enhancement. Med Phys. 2006; 33: 1398-411.

8. Munbodh R, Chen Z, Jaffray DA, Moseley DJ, Knisely JP, Duncan JS. A frequency-based approach to locate common structure for 2D-3D intensity-based registration of setup images in prostate radiotherapy. Med Phys. 2007; 34: 3005-17.

9. Létourneau D, Martinez AA, Lockman D, Yan D, Vargas C, Ivaldi G, et al. Assessment of residual error for online cone-beam CT--guided treatment of prostate cancer patients. Int J Radiat Oncol Biol Phys, 2005; 62: 1239-46.

10. Wang H, Shiu A, Wang C, et al. Dosimetric effect of translational and rotational errors for patients undergoing image-guided stereotactic body radiotherapy for spinal metastases. Int J Radiat Oncol Biol Phys 2008; 71(4): 1261-71

11. Hong TS, Tome WA, Chappell RJ, et al. The impact of daily setup variations on head-and-neck intensity-modulated radiation therapy. Int J Radiat Oncol Biol Phys 2005; 61(3): 779-88

12. Siebers JV, Keall PJ, Wu Q, Williamson JF, Schmidt-Ullrich RK. Effect of patient setup errors on simultaneously integrated boost head and neck IMRT treatment plans. International Journal of Radiation Oncology Biology and Physics 2003; 63: 422-33.

13. Lawson JD, Elder E, Fox T, et al. Quantification of dosimetric impact of implementation of on-board imaging (OBI) for IMRT treatment of head-and-neck malignancies. Med Dosim 2007; 32(4): 287-94

14. Little DJ, Dong L, Levy LB, et al. Use of portal images and BAT ultrasonography to measure setup error and organ motion for prostate IMRT: implications for treatment margins. Int J Radiat Oncol Biol Phys 2003; 56(5): 1218-24

15. Schaly B, Bauman GS, Song W, et al. Dosimetric impact of image-guided 3D conformal radiation therapy of prostate cancer. Phys Med Biol 2005; 50(13): 3083-101

16. Yan D and Lockman D. Organ/Patient geometric variation in external beam radiotherapy and its effect. Med Phys. 2001; 28: 593-602

17. van Herk M, Witte M, van der Geer J, Schneider C, Lebesque JV. Biologic and physical fractionation effects of random geometric errors. Int J Radiat Oncol Biol Phys, 2003; 57: 1460-71.

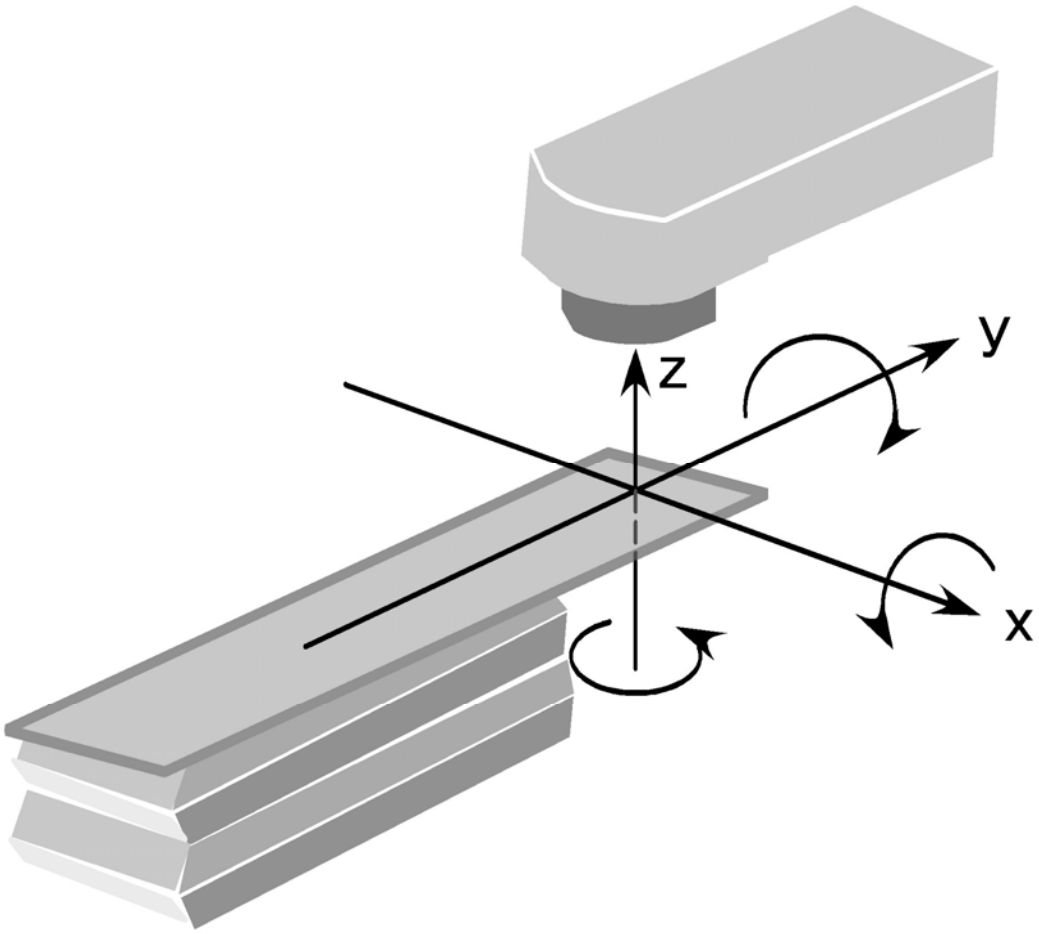

Fig 1 Coordinate system.

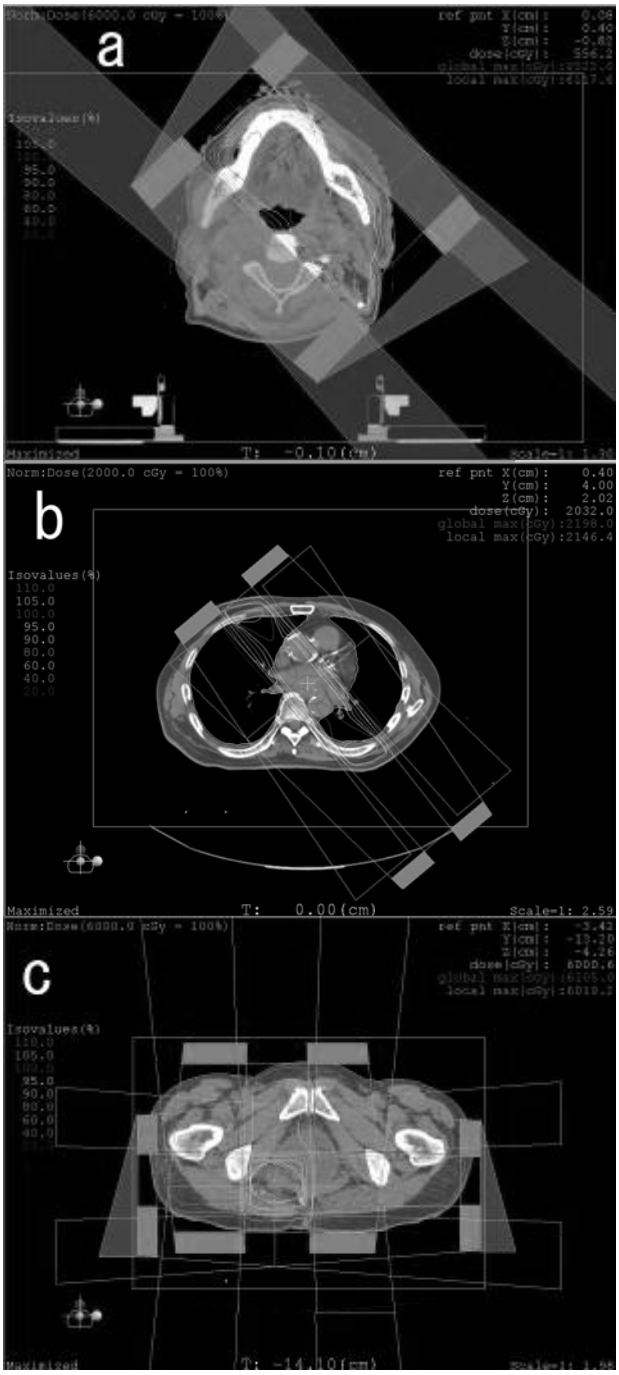

Fig. 2 The original approved plans.

Image a shows the radiotherapy plan for case A, image b shows case B, and image c shows case C.

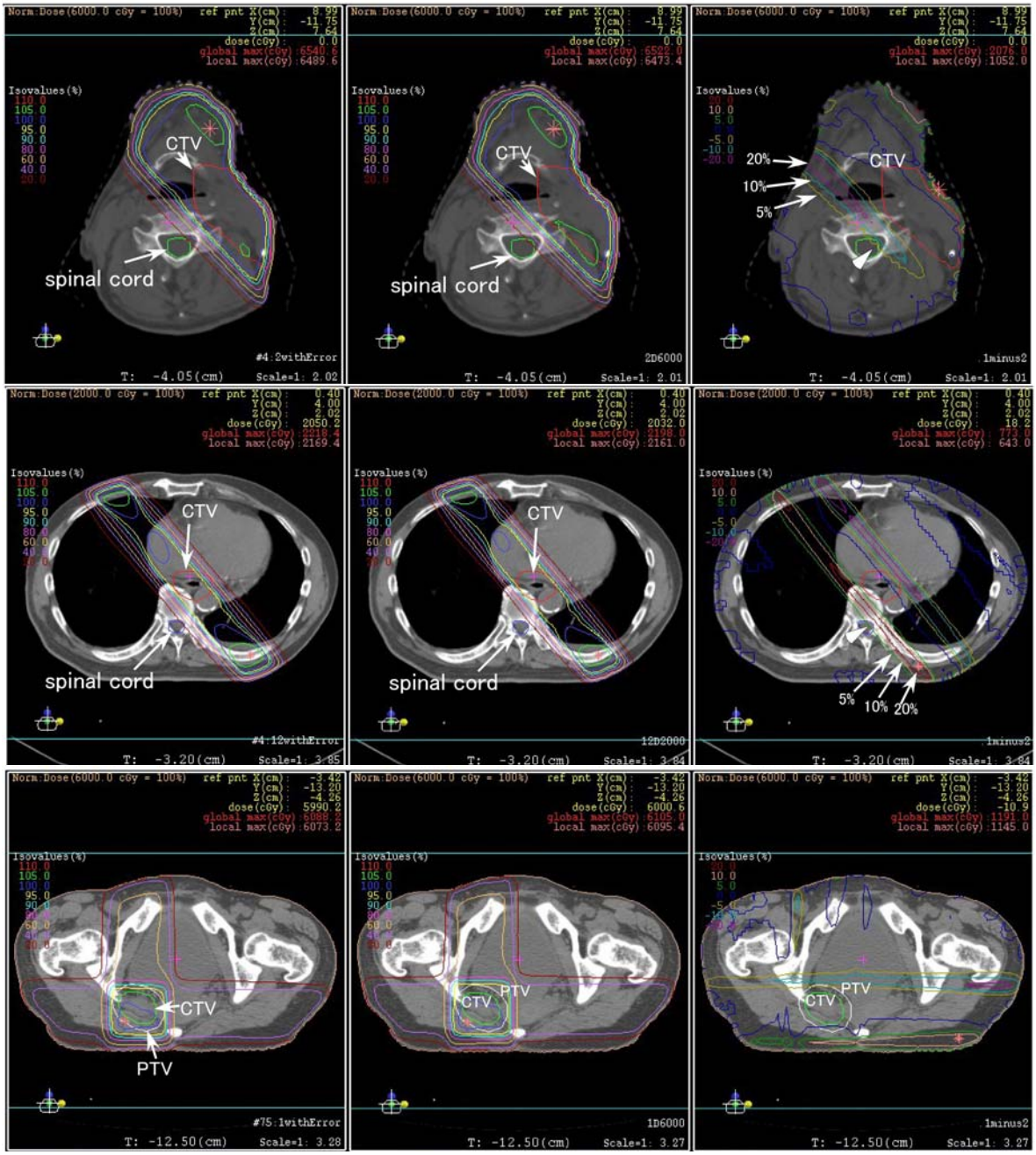

Fig 3　Dose distributions of the plans with setup errors and the original approved plans, and the differential dose distributions.

The top row shows the distributions for case A, the middle row shows the distributions for

case B, and the bottom row shows the distributions for case C. The left column shows the dose distribution of the plan with setup errors, the middle column shows that of the original approved plan, and the right column shows the result of subtracting the dose distribution of the original plan from that of the plan with setup errors. The white triangles indicate the ORs on which iso-dose lines at 5 or 10 % difference were overlapped.

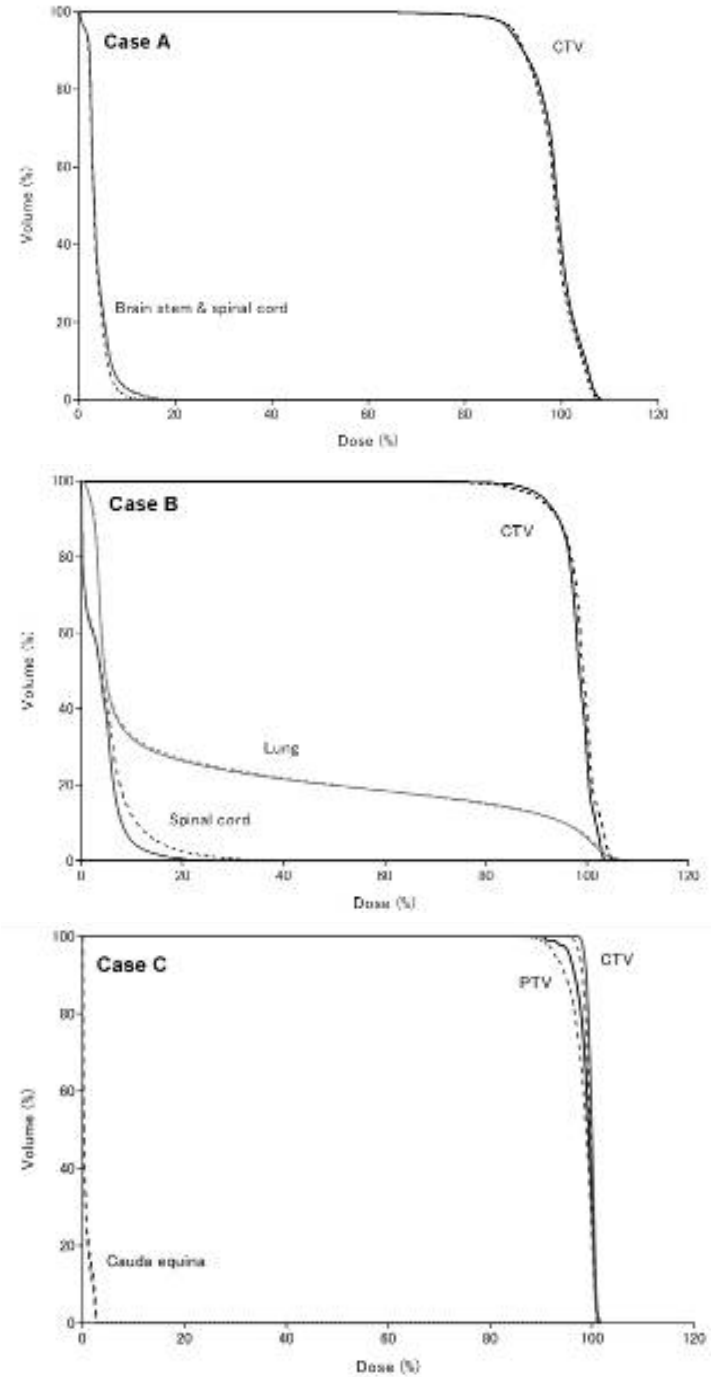

Fig. 4 Dose-volume histograms.

DVHs for cases A, B, and C. Solid lines in all graphs illustrate DVHs in the original approved plan, and dotted lines illustrate DVHs in the plan with setup errors.

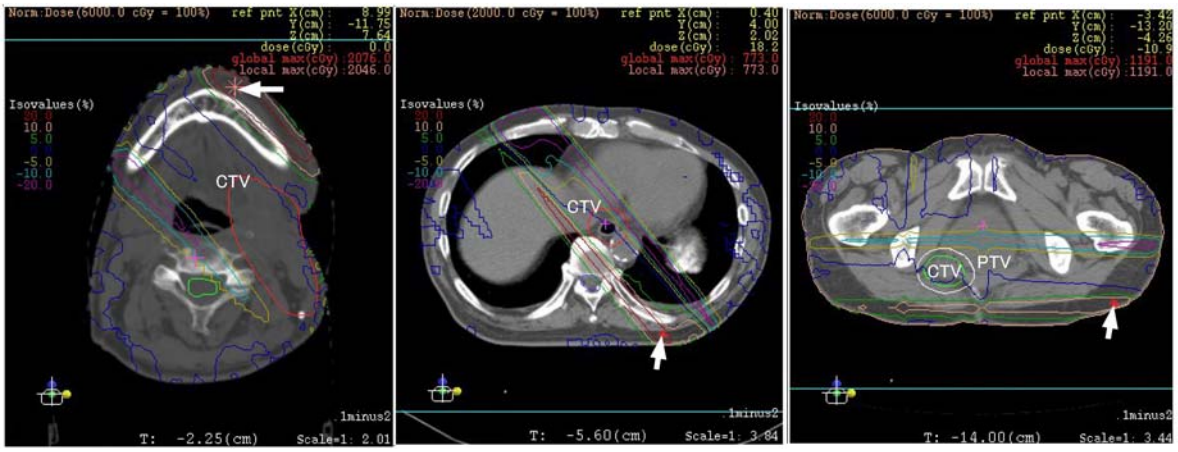

Fig. 5　The maximum dose difference point.

The arrows indicate the position where the dose varied the most. The most varied doses occurred far from the isocenter and near the skin.

Table 1. Summary of cases and setup errors

Case	Age/ sex	Site	Primary	CTV (ml)	Energy (MV)	Beams/ fractions	Total dose (cGy)	Setup error (mean ± SD)	
								Translation (cm)	Rotation (deg)
A	62/M	neck	unknown, LN meta	256.2	6	2/30	6000	X 0.23±0.13 Y -0.16±0.09 Z -0.01±0.13	X -0.45±0.48 Y 2.06±1.21 Z 0.18±0.72
B	74/M	esophagus	esophagus Ca.	192.0	10	2/10	2000	X -0.05±0.25 Y 0.02±0.23 Z -0.22±0.30	X 2.32±0.92 Y 0.08±0.44 Z 0.53±0.96
C	50/F	coccygeal bone	rectum Ca. recurrence	24.1 (59.5)*	10	4/20	6000	X 0.00±0.14 Y -0.19±0.29 Z -0.31±0.26	X-1.61±1.65 Y 1.11±0.77 Z -0.91±0.43

*volume of planning target volume CTV: clinical target volume SD: standard deviation

Table 2. Results of dose distribution difference

Case	Maximum dose difference (%)	Width of 10% iso-dose volume in differential dose distribution (cm)	V95 (%)		Mean dose (%)	
			Approved plan	Plan with setup errors	Approved plan	Plan with setup errors
A	34.7	1.77	82.7	80.6	98.7	98.2
B	35.9	1.85	88.1	88.3	97.9	98.2
C	19.9	1.3	100 (96.8)*	99.9 (89.0)*	99.8 (98.9)*	99.4 (98.1)*

*Values in parentheses are for planning target volume